A sedimentological model to characterize braided river deposits for hydrogeological applications

PETER HUGGENBERGER and CHRISTIAN REGLI

Department of Geosciences, Applied and Environmental Geology, University of Basel, Bernoullistrasse 32, 4056 Basel, Switzerland
(Email: peter.huggenberger@unibas.ch)

ABSTRACT

Braided river deposits form important aquifers in many parts of the world, and their heterogeneity strongly influences groundwater flow and mass transport processes. To accurately characterize these coarse gravelly aquifers, it is important to understand the erosional and depositional processes that form these sediments. Moreover, it is important to evaluate the relative importance of various parameters that determine the preservation potential of different depositional elements over geological time scales. These objectives may be achieved by developing techniques that allow for the integration of different quality data into quantitative models. Information concerning sedimentary textures and the spatial continuity of sedimentary structures in braided river deposits, inherent in depositional facies descriptions, allows the spatial variability of hydrogeological properties (e.g. hydraulic conductivity and porosity) to be predicted. Depositional elements in gravel deposits can contain a restricted range of textures, which form a limited number of sedimentary structures. These depositional elements are bounded by erosional and/or lithological surfaces. The frequency, size and shape of different elements in a sedimentary sequence depend on several factors, including aggradation rate, channel belt mobility on the kilometre scale, gravel-sheet/scour activity at the scale of hundreds of metres and topographic position of the different elements within an evolving system. Preserved shape and size of the elements affect the correlation lengths and the standard deviations of the aquifer properties, such as hydraulic conductivity and porosity.

Different quality data sets that may be used in characterizing braided river deposits can be recognized in outcrop, boreholes and on ground-penetrating radar (GPR) sections. This paper proposes a means of integrating outcrop, borehole and GPR data into a stochastic framework of sedimentary structures and the distribution of hydraulic aquifer properties. Data integration results in variable degrees of uncertainty when assigning values to hydraulic properties and characterizing the geometry of sedimentary structures. An application of this approach is illustrated using a data set (400 m $\times$ 550 m) from the northeastern part of Switzerland at the confluence of the Rhine and Wiese rivers. The data set includes drill-core data from five boreholes and 14 GPR sections with a total length of 3040 m. The results of the variogram analysis provide the orientation of sedimentary structure types representing the main flow direction of the River Rhine in the lower part of the aquifer, and of the River Wiese in the upper part. The analysis also results in large ranges of spatial correlation, ranging from a few metres up to tens of metres for the different sedimentary structure types.

Keywords Gravel heterogeneity, sedimentological model, stochastic modelling, groundwater.

INTRODUCTION

A large proportion of European and North American aquifers were formed by former braided river systems. Accurate predictions of groundwater flow and transport behaviour within these sediments rely on detailed knowledge of the distribution of physical, chemical and biological aquifer properties. The complexity of depositional and erosional processes in braided river systems, however,

leads to highly heterogeneous distributions of hydrogeological parameters such as hydraulic conductivity and porosity. Hydraulic conductivity variations over several orders of magnitude are of primary importance in groundwater flow and solute migration (Gelhar, 1986; Adams & Gelhar, 1992; Rehfeldt *et al.*, 1993). Due to the complexity of the aquifer structures in these coarse gravelly deposits, and its consequences for hydraulic property distribution, stochastic modelling has rarely been applied to practical problems (Dagan, 2002).

Continuous three-dimensional information on the hydraulic properties of aquifers cannot be obtained easily in heterogeneous sediments. Consequently, different methods have been developed in order to map aquifer properties. Koltermann & Gorelick (1996) distinguished three main types of methods: (1) structure-imitating methods that use any combination of Gaussian and non-Gaussian statistical and geometric relationships in order to match observed sedimentary patterns; (2) process-imitating methods that consist of both aquifer calibration techniques, which solve the governing equations of fluid flow and transport, and geological process models that combine mass and momentum conservation principles with sediment transport equations; and (3) descriptive methods that use different field methods to translate geological facies models into hydrofacies models with characteristic aquifer properties.

All these methods have already been applied in coarse fluvial gravel deposits that are typical of braided river environments. Examples of each approach, including key information for the understanding of sedimentological facies description and aquifer characterization, as cited in the literature, are provided below.

1 Structure-imitating methods: Jussel *et al.* (1994) developed unconditioned, Gaussian stochastic models of glacio-fluvial deposits using statistical data derived from outcrop descriptions of gravel pits in northeastern Switzerland. Facies interpretations obtained from ground-penetrating radar (GPR) profiles by Rauber *et al.* (1998) from one of these gravel deposits (Hüntwangen, Switzerland) were used to condition stochastic models. Both groups of authors used their stochastic models to simulate a synthetic tracer transport experiment. Among non-Gaussian methods, indicator-based simulations offered the advantage of combining different types of observations, using 'hard' and 'soft' data (e.g. McKenna & Poeter, 1995). Regli *et al.* (2004) developed the software code GEOSSAV, which is capable of incorporating these different data types by including drill-core descriptions and GPR profiles, to produce a stochastic model that could be tested against tracer breakthrough responses in the 'Langen Erlen' well catchment zone (Regli *et al.*, 2003).

Other non-Gaussian approaches include Boolean, or object-based methods, which are suited to randomly distributed sedimentary body shapes that are typical of fluvial deposits (Deutsch & Wang, 1996). Geological information has been used to develop geometrical and probabilistic rules that control the distribution, geometry, elongation axis and connectivity for each of the simulated objects or facies types. Another promising non-Gaussian approach has explored the influence of aquifer structure on groundwater flow regimes using transition probabilities (Markov chains; Carle *et al.*, 1998; Fogg *et al.*, 1998). Weissmann *et al.* (1999) presented a Markov chain geostatistical approach to create geologically plausible three-dimensional characterizations of a heterogeneous, fluvial aquifer system. The maps were conditioned using core, well-log and soil data from the Kings River alluvial fan aquifer system in California. Using this approach, pattern-imitating methods have simulated the architecture and lithology of fluvial deposits directly, based on geometric concepts of the observed geology. Webb (1994) and Webb & Anderson (1996) presented a simulation method that develops the three-dimensional distribution of sediment units in braided stream deposits. Their code, BCS-3D, combines a random-walk algorithm for braided topological networks with equations to describe hydraulic channel geometry, which were then used to estimate the channel shape and connectivity relations of a surface. Sediment aggradation in the third (vertical) dimension was obtained by stacking the generated geomorphological braided river surfaces using a constant offset, and the resulting sedimentary model was used to assign distributed hydraulic conductivities.

2 Process-imitating methods have not been used extensively for modelling fluvial sediments. Koltermann & Gorelick (1992) used large-scale process simulations to reconstruct the geological

evolution of an alluvial fan in northern California over the past 600,000 yr. The reconstruction of the Alameda Creek fan highlighted the importance of climate change, tectonics and relative sea-level change on the depositional processes. Nonetheless, geological process models have rarely been applied to hydrogeological problems, largely because they use initial and boundary conditions that are largely unknown and consequently cannot be conditioned to measured values.

3 Descriptive methods produce maps of the architecture of fluvial deposits by the translation of geological or geophysical site-specific data into conceptual facies models. The quality of field observations is of prime importance. Lithofacies concepts of braided river deposits have been developed by Allen (1978), Miall (1985), Brierley (1991), Paola *et al.* (1992), Heller & Paola (1992), Bridge (1993, 2003) and Siegenthaler & Huggenberger (1993). Ashmore (1982, 1993) and Ashmore & Parker (1983) have demonstrated the importance of key elements such as braiding intensity and scouring on sedimentation using laboratory experiments and field observations of braided river systems (Bridge, 2003; Ashworth *et al.*, 1999, 2004). Anderson (1989) and Klingbeil *et al.* (1999) related the concept of lithofacies to hydrofacies in a fluvial environment, and Anderson *et al.* (1999) used extensive outcrop observations and sampling information for hydrofacies conceptualization. Generally, outcrops and boreholes offer a restricted image of the sedimentary architecture and grain-size distribution data. The additional application of shallow geophysical methods such as high-resolution GPR has been shown to be very effective in mapping the relevant hydrofacies (e.g. Huggenberger, 1993; Bridge *et al.*, 1995; Best *et al.*, 2003). Lunt *et al.* (2004) combined GPR surveys with data from trenches, cores, logs, and permeability and porosity measurements in a study of a three-dimensional depositional model of the Sagavanirktok River in Alaska. Techniques used in three-dimensional surveying offer the possibility of generating images of the spatial structure of fluvial aquifer architecture on a decimetric scale (Beres *et al.*, 1995, 1999; Asprion & Aigner, 1999; Heinz, 2001). Regli *et al.* (2002) coupled probability estimations of drill-core descriptions to radar facies types to define sedimentary structure types for the Langen Erlen aquifer.

Various braided river system depositional models are controversially debated in the literature. Controversies have arisen mainly as a result of the difficulty in finding simple relationships between morphological elements observed in modern braided river systems and the geometry of architectural elements of ancient braided river deposits. Such relations can be based only on two-dimensional outcrop observations combined with two-dimensional and three-dimensional GPR data sets that provide data to a limited depth, in conjunction with certain concepts concerning the preservation potential of former morphological elements in the sedimentary record. The prediction of the architecture of braided river deposits cannot be based on observations of recent braided river system morphology at low flow stage alone, since structures developing under very high flow conditions (catastrophic or landscape shaping events) give better information on the spatial extent of characteristic depositional elements. In terms of hydrogeological applications, it is important to remember that conceptual sedimentological models are based on their relevance to groundwater hydraulics. There are many indications from hydrogeological investigations (e.g. Flynn, 2003) that the role of highly permeable sediments, such as open-framework gravel, is often underestimated.

The objective of this paper is to derive a methodology to characterize braided river deposits for hydrogeological applications by using different quality geological information. This includes:

1 definition of sedimentary textures, structures and depositional elements together with a discussion of the links between surface morphology and the subsurface sedimentary structures;
2 presentation of a method by which outcrop, borehole and GPR data can be integrated in a structure-imitating aquifer model;
3 presentation of a case study of the application of subsurface modelling for the Rhine/Wiese sand and gravel aquifer near Basel, Switzerland (Fig. 1).

The stochastic simulations characterize possible spatial distributions of aquifer properties that can be used as an input for groundwater flow and transport simulations.

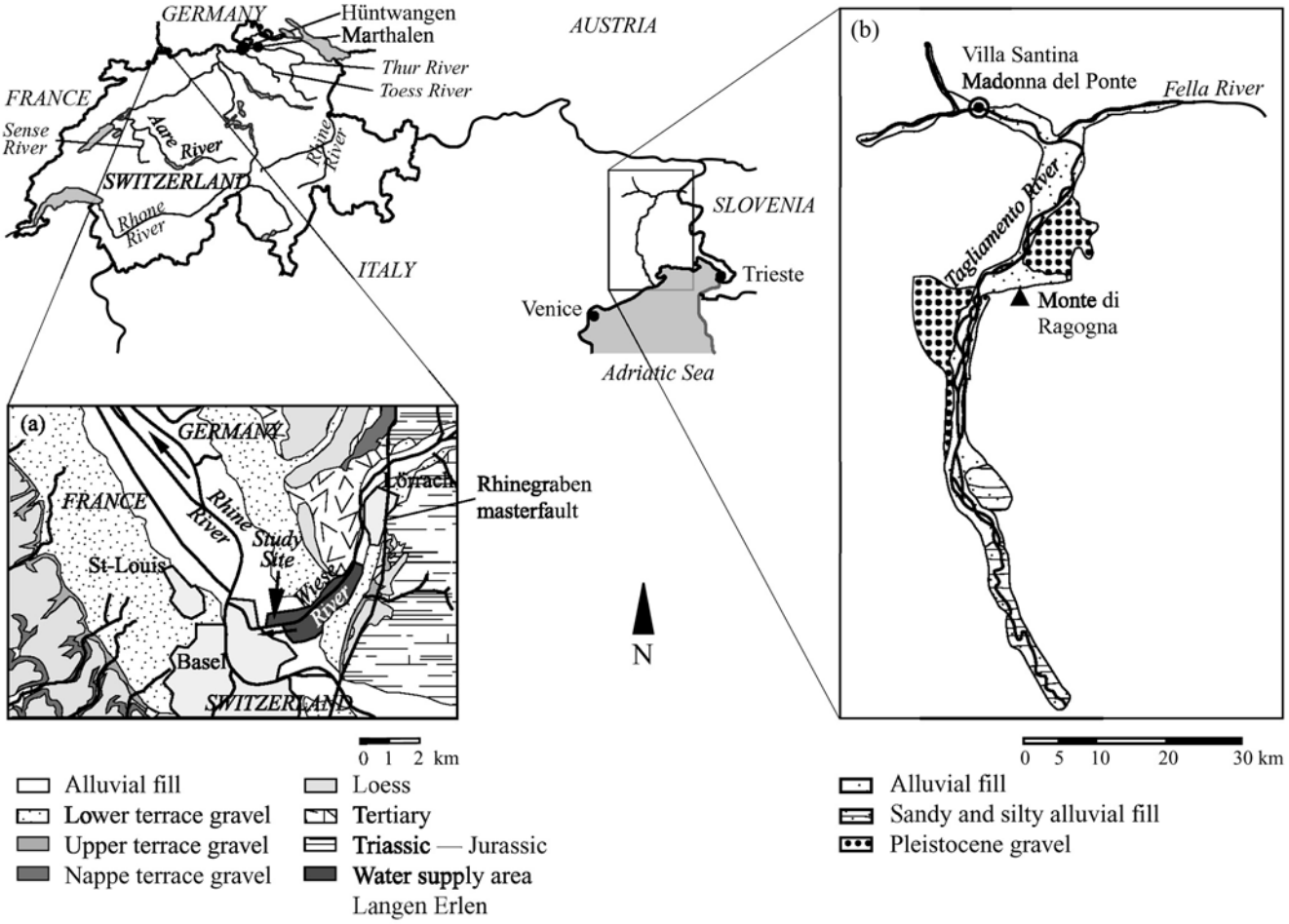

Fig. 1 Locality map of rivers and outcrops cited in the text. Insets show: (a) simplified geological overview of the Basel area (Switzerland) including the location of study site in the Basel water supply area (Langen Erlen), located within the ancient confluence of the River Rhine and River Wiese; (b) overview of the Tagliamento area, Friaul, northern Italy.

METHODS

In order to refine sedimentological models to permit characterization of braided river deposits to be extended to hydrogeological applications, different methods for modelling aquifer sedimentology and the subsurface have been applied. Following the hydrogeological facies concepts of Asprion & Aigner (1999), sedimentary textures, structures and depositional elements were defined. The preservation potential of depositional elements, and its significance for groundwater flow and transport in their influence on hydraulic conductivity and porosity, are used as key information in this type of classification. Important information was obtained by comparison of morphological elements, observed at the surface of modern braided river systems (e.g. River Tagliamento, Friaul, northeastern Italy), with preserved depositional elements that were investigated in gravel pits deposited by the Pleistocene Rhine River in Switzerland (Fig. 1). Moreover, the results from laboratory flume experiments, numerical models, field measurements and proposed fluvial processes (e.g. fluvial sediment sorting processes) can form the sedimentological facies relations described (Ashmore, 1982, 1993; Klingemann & Emmet, 1982; Van Dyke, 1982; Carling & Glaister, 1987; Carling, 1990; Tubino *et al.*, 1999; Lanzoni, 2000).

Outcrop, borehole and GPR profiles represent data of different quality. Outcrop and laboratory investigations of representative samples concerning facies or hydraulic properties provide the

most reliable data, and are considered as *hard data*. In contrast, drill-core and GPR data are less precise and considered to be *soft data*, and greater uncertainties are associated with these data values. The differences between hard and soft data required an interpretation method to be developed that allowed the integration of different quality datasets into proposed lithofacies schemes. The method provides probabilities that drill-core layer descriptions and radar facies types represent particular defined sedimentary structures.

Accurate modelling of subsurface parameter distributions becomes progressively more difficult with increasing heterogeneity and uncertainty in the spatial variability of available data. Uncertainty depends both on the quantity and the quality of available data. Stochastic simulation as described below implies sampling from conditional distributions, and the resulting spatial models consist of samples from a multivariate distribution characterizing the spatial phenomenon. The sequential indicator-based approach matches the sedimentary structures using conditioning data, such as drill-core and GPR information, with the spatial correlation of data values, depending on the sedimentological model as described in the following sections, and the geostatistical analysis of the available data verified in variogram analyses.

SEDIMENTARY TEXTURES, STRUCTURES AND DEPOSITIONAL ELEMENTS

Based on outcrop analyses of gravel pit exposures of sediments deposited during the Pleistocene by the Aare, Rhine, Rhône and Thur rivers in Switzerland (Fig. 1), and established facies schemes (Siegenthaler & Huggenberger, 1993; Jussel *et al.*, 1994; Rauber *et al.*, 1998; Regli *et al.*, 2002), a limited number of textural and structural sediment types, reflecting dominant depositional elements developing in braided river systems, were defined.

Sedimentary texture and structure types

Definition of sedimentary texture types is based on grain-size distribution and sediment sorting. In the Rhine gravel, sedimentary textures are easily recognizable in outcrop due to colour variations caused by the presence or absence of sand-fractions, silt and clay and the wetting/drying characteristics at the outcrops. Consequently, colour is used in field classifications of different gravel textures (Jussel *et al.*, 1994). Bearing in mind that colour differences are dependent on the source rock material, the sedimentary textures are considered as an important attribute in distinguishing different sedimentary structures in outcrop; such textures are also frequently used in drill-core descriptions. Investigations at different field locations and subsequent data interpretation allow the classification of seven different sedimentary texture types (Fig. 2a–g).

1 Open-framework gravel (OW, Figs 2a & 3a, c) is a well-sorted gravel, in which pore space is free of sand and silt, although clay and silt particles occasionally drape the pebbles and cobbles. Mean grain-size (d_m) and sorting coefficient ($s_c = d_{60}/d_{10}$) for OW are 0.015 m and 3.3, respectively (s_c corresponds to the slope of the grain-size distribution curve between d_{10} and d_{60} and is an indicator of sediment sorting (Swiss Standard Association, 1997)). Open-framework gravel corresponds to a well-sorted, poorly graded (high porosity) sedimentary texture type.
2 Bimodal gravel (BM, Figs 2b & 3a, c) consists of a matrix of well-sorted medium sand that fills interstices of a framework of well-sorted pebbles and occasional cobbles (d_m = 0.021 m, s_c = 77). Visual inspections of BM in outcrop give the impression that the grain-size and bed-thickness of BM are positively correlated (see also Steel & Thompson, 1983).
3 Grey gravel (GG, Figs 2c & 3b, d–f) is a poorly sorted gravel, containing coarse sand, granules, pebbles and, rarely, cobbles. Clay and silt particles never make up more than 5% of the deposit (d_m = 0.007 m, s_c = 55).
4 Brown gravel (BG, Figs 2d & 3d–e) is a poorly sorted gravel with sand and silt (d_m = 0.021 m, s_c = 236).
5 Silty gravel (SG, Fig. 2g) is a poorly sorted, brownish coloured, gravel, often containing up to 30% sand and nearly 20% silt and clay (d_m = 0.002 m, s_c = 250).
6 Sand lenses (SA, Fig. 3f) may be poorly sorted to well-sorted and do not contain significant silt or clay fractions.
7 Silt lenses (SI, Fig. 2f) consist of a poorly graded silt.

Sedimentary structure types are made up of one or a combination of two sedimentary texture

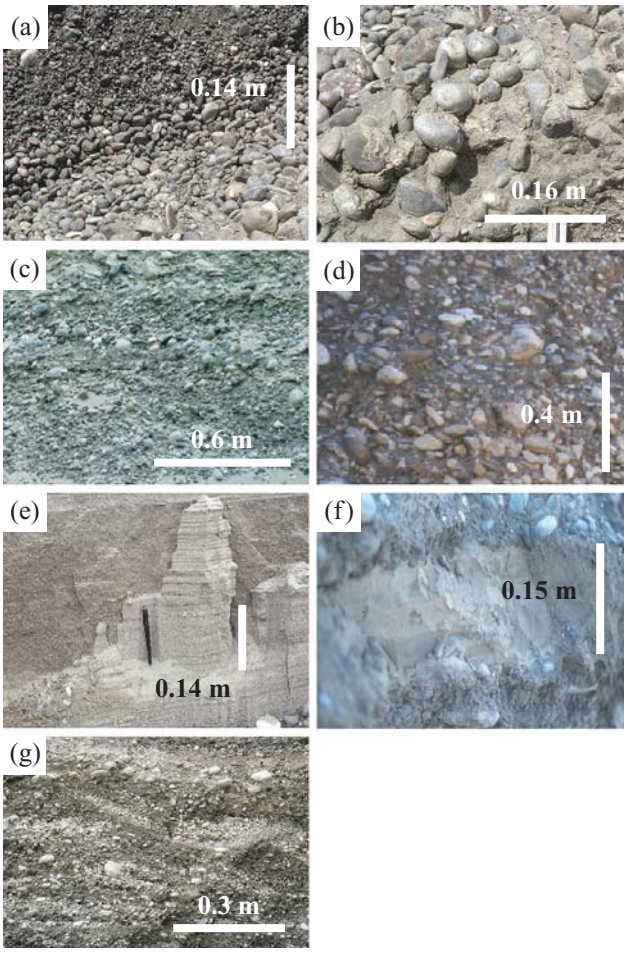

Fig. 2 Sedimentary textures types: (a) (OW) open-framework well-sorted gravel; (b) (BM) bimodal gravel; (c) (GG) poorly sorted, clean grey gravel; (d) (BG) poorly sorted, coarse brown gravel with silt fraction; (e) (SA) sand; (f) (SI) silt; (g) (SG) silty gravel. Photographs (a–c) and (e–g) from Pleistocene Rhine gravel at Hüntwangen, (d) from Sense River, Switzerland.

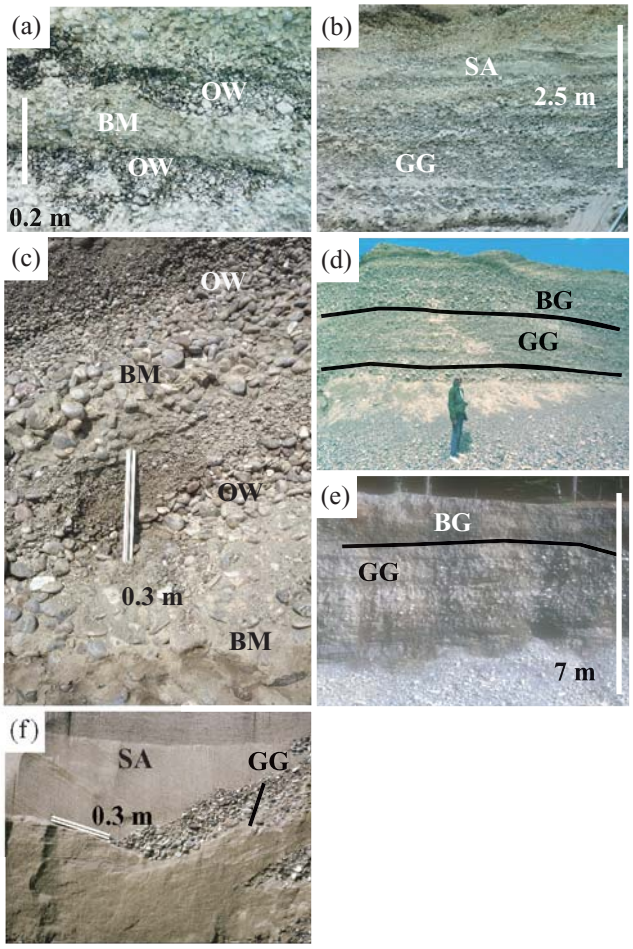

Fig. 3 Sedimentary structures types: (a), (c) (OW/BM) open-framework well-sorted/bimodal gravel couplet consisting of BM at the base and OW at the top; (b), (f) alternating beds of SA/GG; (d), (e) GG/BG and SG/GG. All samples from Pleistocene Rhine gravel, Hüntwangen, Switzerland.

types that may alternate. The seven sedimentary texture types identified may be grouped into nine sedimentary structure types (Fig. 3).

1 OW appears in fining upward beds that are one to several decimetres thick, and individual clasts are not oriented.
2 OW/BM couplets are fining-upwards sequences consisting of BM at the base and OW at the top. A transition from BM to OW is generally marked by a sharp boundary between the sand in the BM and the open pores of the OW. The pebbles, however, show a continuous fining-upwards sequence from BM to OW.
3 GG often forms thick sheets of poorly sorted sediments up to 2 m thick.
4 The bedding of BG is massive, and often forms beds up to 4–6 m thick.
5 & **6** GG and BG may also occur in alternating layers that are either horizontal (GG/BG-h) or inclined (GG/BG-i).
7 SG may occur in close relation to BG, as massive beds or associated with thin silt layers. However, the latter are not very frequently observed in outcrop.
8 SA may occur in different settings on a floodplain and with varying proportions of GG and SI.

9 SI mainly occurs as thin beds or near the top of gravel sequences, sometimes associated with gravels in smaller trough-shaped fills.

Depositional elements

Depositional elements (Fig. 4a–f) are defined based on the geometrical form of erosional and/or lithological boundaries and the character of the fill (e.g. structure types and geometry of planar or tangential foresets). The most abundant elements in the deposits investigated are: (1) scour or trough fills (Fig. 4d–f); (2) gravel sheets or gravel dunes that usually form thin gravel layers, although these may be up to more than 1 m thick (Fig. 4a, c); (3) bedload sheets (Fig. 4b, c) or traction carpets (Todd, 1989); and (4) overbank deposits (Siegenthaler & Huggenberger, 1993; Beres *et al.*, 1999, fig. 3; Heinz, 2001).

1 Scour or trough fill deposits (Figs 3–5) can be composed of four different sedimentary structure types: (i) sets with OW/BM couplet cross-beds; (ii) sets with GG cross-beds; (iii) sets with SA cross-beds; and (iv), in the braided–meandering transition zone (which is marked by a decrease in slope and widening of the floodplain to the west of the Rhinegraben masterfault), sets with SG cross-beds (Regli *et al.*, 2002). The cross-bedded sets are 0.1–0.5 m thick with trough-shaped, erosional concave-upward lower bounding surfaces. The erosional surface appears as a clear boundary that is discontinuously overlain by a lag of cobbles in some outcrops. In sections approximately perpendicular to the general flow direction, the erosional bounding surfaces may display the shape of circular arc segments, while the cross-beds are strongly curved and tangential to the lower set boundary (Huggenberger *et al.*, 1988).
2 Horizontally bedded gravel sheets (Fig. 4a, c) mainly consist of GG with occasional alternations with single beds of BG. Individual beds range in thickness from <0.1 m to about 1 m thick, but are typically 0.1–0.3 m thick. Very thick beds are probably obscure low-angle cross-stratified sets. Single beds extend laterally from a few metres up to several tens of metres. The bedding is mostly vague and caused by: (i) variable sand fractions especially within the GG; (ii) vertical alternations of different textural types; (iii) thin interlayers of sand and pebbles; or (iv) discontinuous stringers or coarse pebbles and cobbles.

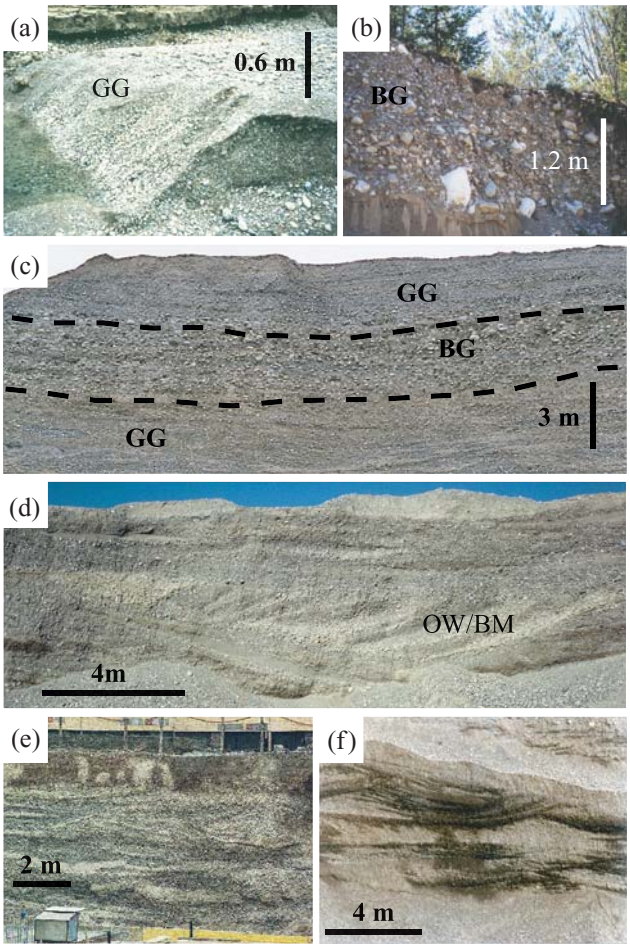

Fig. 4 Depositional elements: (a), (c) gravel sheets (a, flow from right to left, River Toess; c, section perpendicular to ancient mean flow direction, Pleistocene Rhine gravel, Hüntwangen); (b) bedload sheet (River Sense, Switzerland); (d–f) scour and trough-fill deposits (sections perpendicular to ancient mean flow direction, all outcrops from Pleistocene Rhine gravel; d, Hüntwangen, e, Basel, f, Marthalen). Note the concave-upward trough-shape and erosional lower bounding surfaces. Trough-fill deposits (d) consist of tangential bottom sets with gravel couplet cross-beds. (GG) Grey gravel; (BG) poorly sorted, coarse brown gravel with silt fraction; (OW/BM) open-framework well-sorted/bimodal gravel couplet.

3 Laterally extensive, massive and coarse-grained gravel sheets (Fig. 3d, e) are composed of BG. Single beds or sets of beds have thicknesses ranging from decimetres up to several metres. Laterally, thickness may vary abruptly and the beds may locally disappear or reduce to a discontinuous lag of coarse cobbles. A preferred orientation or imbrication of the clasts

Fig. 5 Pleistocene trough-fill dominated sequence in Rhine gravels at Marthalen, Switzerland, in a section perpendicular to the mean ancient flow direction. Note the dominance of filled trough structures and the absence of gravel-sheets. Type OW/BM makes up to more than 60% of the whole sequence.

is quite common, and the long axis of the clasts usually dips approximately 15° upstream.
4 Overbank deposits are composed of SA and SI and, compared with the active channel area, fine-grained sediments (fractions finer than fine sand) are more abundant. Floodplain deposits consist of massive to horizontally bedded medium to coarse silt and very fine sand, and in a few examples fine sand. Bioturbation may be intense in more recent sediments, and is mainly due to rooting by abundant vegetation. In Pleistocene sequences, however, only a small amount of organic matter may be observed due to the lack of a plant cover. Sandy beds with ripples or parallel laminae often occur near the active channel belt, mainly as a product of moderate to high magnitude floods (Huggenberger *et al.*, 1998).

Relationship between depositional elements of ancient rivers and morphological elements of modern braided river systems

It is often difficult to estimate the maximum dimensions and orientation of depositional elements of braided river deposits preserved in the geological record. Although voluminous information is available from photographs of progressively excavated terrace walls (Jussel, 1992; Siegenthaler & Huggenberger, 1993), the maximum dimensions of depositional elements are commonly impossible to ascertain without two-dimensional and three-dimensional GPR data sets. Moreover, the results of a three-dimensional GPR study of a 70 m × 120 m × 15 m block have demonstrated that the dimensions of depositional elements such as trough fills can be significantly larger than the size of the block investigated (Beres *et al.*, 1999).

Observations of morphological elements on the floodplain of the Tagliamento River (Fig. 1) immediately after a moderate magnitude flood ($2000\ m^3\ s^{-1}$) allowed study of both the geometrical form and extent of gravel sheets (Fig. 6) and the simultaneous progradation of a gravel sheet with the development of a scour fill in front of the gravel sheet (Fig. 7). This flood has allowed some important products of the high-flow stage to be documented that are generally overprinted by smaller events, such as development of smaller gravel sheets, or which are not accessible to observation (e.g. processes in scours). There are few examples documenting simultaneous gravel-sheet and scour development in rivers. However, Fay (2002) documented trough-shaped scour fills and related them to the November 1996 glacier-outburst flood, Skeidarársandur, southern Iceland. Their scour-fill geometry (Fay, 2002, fig. 9) strongly resembles structures found in the Rhine gravel deposits of northeastern Switzerland (Siegenthaler & Huggenberger, 1993, fig. 6).

Gravel sheets

The geometry of two gravel sheets that are more than 200 m long and 80 m wide is documented in Fig. 6. The gravel sheets are in concordance with the previous riverbed topography and developed at moderate magnitude flow, where the active channel belt was wholly inundated and the morphology of the floodplain was reshaped. The orientation of the longitudinal direction of the gravel sheet differs from the orientation of the channels developing at the end of a flood event. Irregularly sinuous, single-thread channels, including channel islands, dominate the morphological character of the fluvial system at low flow, and the angle between the longitudinal directions of the gravel sheets varies according to the intersection with these channels. In the present example, the angle is ~20–30°. This difference in transport direction marks the difference between the braiding character of the river system during flooding and

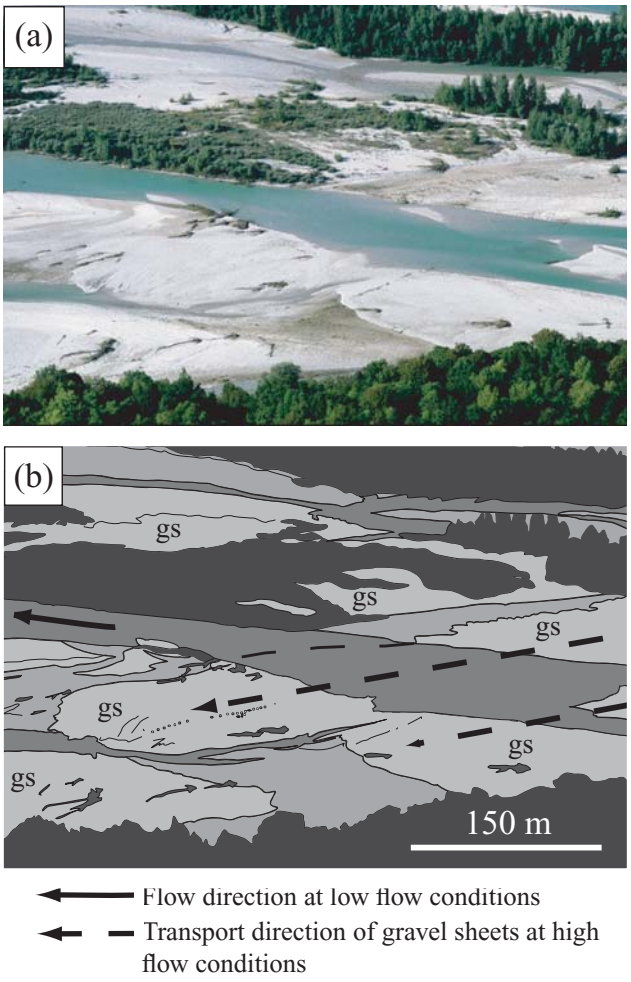

Fig. 6 Observations of modern river analogues: (a) photograph and (b) interpretation of a view of the Tagliamento River from Monte di Ragogna (Friaul, Italy). Flow from right to left. Note the angle between the active channels under low-flow conditions and the long axis of gravel sheets (gs) developed during flood (high-flow) conditions. The low-flow channel in the central part of the photograph dissects the gravel sheets.

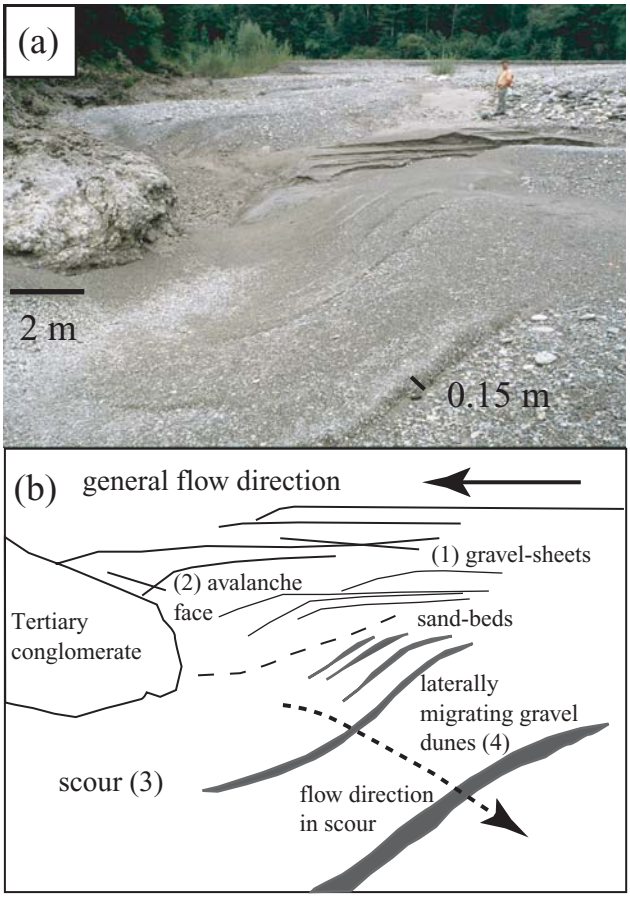

Fig. 7 Observations of modern river analogues: (a) photograph and (b) interpretation of relics developed by a scour-fill process at Madonna del Ponte, Villa Santina (Friaul, Italy). The photograph provides a three-dimensional view of a river section abandoned immediately after a flood event. The mean flow direction in the channel is from right to left. Within the scour, smaller gravel dunes have migrated across the lateral wall of the scour. Note the difference in elevation between the top of the gravel sheets and the deepest part of the scour pool (approximately 6 m). Gravel sheets (1), avalanche faces (2), transition zone to scour pool (3) and upward migrating gravel dunes (4) developed simultaneously.

the channels at low-flow conditions (Leopold & Wolman, 1957; Church, 2002).

Simultaneous gravel-sheet and scour development

Whereas gravel sheets are at least partly preserved after floods (Lunt *et al.*, 2004, fig. 6), scours and related trough fills developing simultaneously during gravel-sheet propagation (Ashmore, 1982) are filled up with sediment deposited with declining flood energy. As trough fills are buried below the upper units of a fluvial channel, they generally can be portrayed only on GPR profiles (Huggenberger *et al.*, 1998). The development of sedimentary structures within a scour was observed at Madonna del Ponte (Villa Santina, Friaul, Fig. 1) immediately after a flood in 2000. Figure 7 gives a view perpendicular to the mean flow. The avalanche faces in front of the gravel sheets or dunes mark a transition from gravel sheets to the scour, the

erosional base of which is at least 3–4 m below the top of the gravel sheets. Such transitions represent negative steps that can lead to the development of flow separation zones (Allen, 1984), which favour sediment sorting, such as cross-bedding and the development of gravel couplets (Carling & Glaister, 1987). In the scour itself, gravel dunes have been observed migrating across the lateral trough wall. Along the individual dune front (step), cross-bed sets with completely obscured foresets develop (e.g. Siegenthaler & Huggenberger, 1993, fig. 5). The maximum amplitude of the dune crests is in the order of 0.1–0.2 m. While the model of Carling & Glaister (1987) can explain planar, cross-bedded gravel couplets (OW/BM), this particular example from the Tagliamento River could illustrate the formation of tangential gravel couplets (e.g. Fig. 4d).

HYDROGEOLOGICAL CHARACTERIZATION OF BRAIDED RIVER DEPOSITS

Hydraulic properties of sedimentary structure types

The hydraulic properties of different sedimentary structure types have been determined from slightly or undisturbed sediment samples taken of individual sedimentary texture types from outcrops in the unsaturated zone (Huggenberger *et al.*, 1988; Jussel *et al.*, 1994). The results of hydraulic testing and geostatistical analysis display significant differences in the hydraulic properties of the different sedimentary structure types in comparison with the variability of the individual texture types. The mean and standard deviation of the measured hydraulic conductivities in unsaturated or slightly disturbed samples (Rauber *et al.*, 1998) indicate that the effect of OW structures (geometric mean of hydraulic conductivity, K, 1×10^{-1} m s^{-1}; standard deviation of the natural logarithm of K, $\sigma_{\ln K}$, >0.8) on the groundwater velocity distribution is much more important than the influence of admixtures of other sedimentary structure types (K, 1×10^{-3} to 1×10^{-5} m s^{-1}; $\sigma_{\ln K}$, 0.4–0.8). The frequency of occurrence and the dimensions of the OW strata determine the correlation length and the standard deviation of the hydraulic conductivity in coarse gravel deposits. Stauffer & Rauber (1998) showed that OW strata in OW and OW/BM structures dominate these statistical parameters of the gravel deposits, although their total volumetric fraction was quite small (2.8%).

Recognition of sedimentary structure types from drill-core and GPR data

Outcrop, drill-core and geophysical information represent data of different quality and resolution at different scales. Due to the easy access and visibility of undisturbed sedimentary structures and textures, outcrop investigations provide very reliable hard data. Unfortunately, few outcrops are available for studies. Drilling may destroy sedimentary structures and can smear the interface with adjacent layers. Typically, drill-core layer descriptions are not very detailed and do not clearly indicate explicit texture or structure types, even if grain-size analyses are available (e.g. overlapping ranges of grain-size distributions of different sedimentary texture types; Jussel, 1992, fig. 2.5a–d). In addition, the quality of individual drill-core descriptions varies considerably depending on the geotechnical or sedimentological approach used. Consequently, drill-core data are normally considered as soft data.

Non-destructive GPR techniques permit depositional elements and sedimentary structures to be delineated based on the geometry of the bounding surfaces and on smaller internal reflections. However, the relationship between reflection patterns and sedimentary structure types is frequently ambiguous, and consequently the results of GPR studies are also considered as soft data.

The concept of recognizing sedimentary structure types using drill-core and GPR data is based on the lithofacies scheme developed for the Rhine gravel, described in Siegenthaler & Huggenberger (1993), Jussel *et al.* (1994), Rauber *et al.* (1998) and Regli *et al.* (2002). Drill-core and GPR data have also been interpreted and integrated into this lithofacies scheme (Fig. 8). The data interpretation includes a probability estimate that drill-core layer descriptions and reflection patterns represent defined sedimentary structure types.

Interpretation of drill-core data

Sedimentological drill-core descriptions of coarse gravel deposits provide information on the com-

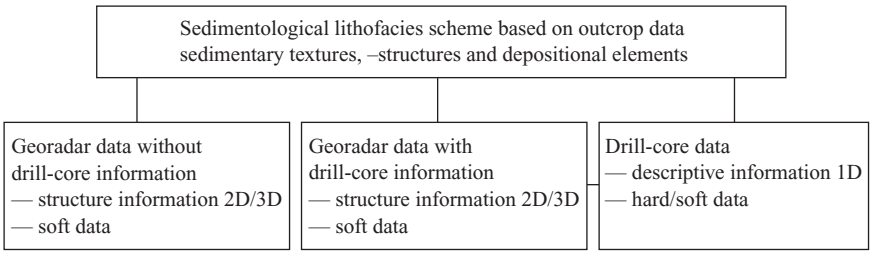

Fig. 8 Classification and integration of different quality data for characterizing braided river deposits.

position and texture of deposits. More specifically, details of grain-size categories, sorting, major constituent composition and the proportion of each grain-size fraction can be determined, as well as information about the colour, chemical precipitation, thickness of a deposit and its transition with the underlying layer (Table 1). Based on these data, the probability can be estimated that a drill-core layer description represents a defined sedimentary structure type (structure-type probability). The estimation of probability and the mathematical details of this method are described in Regli *et al.* (2002).

Differentiation of the probabilities of the sedimentary structure types follows an iterative process, whereby each type of information is considered. The iterative differentiation of sedimentary structure-type probabilities is illustrated using the example presented in Fig. 9 (Rhine/Wiese aquifer, Fig. 1). A drill-core layer described as grey, clean, poorly sorted gravel, with abundant medium and coarse sand, abundant pebbles and cobbles, normal thickness (0.25–2.5 m), and underlain by a layer of rather silty gravel, contains information (see Table 1) that allows the differentiation of the single structure-type probabilities. Starting with the initial probability values for sand, gravel, pebbles and cobbles (Regli *et al.*, 2002, table 2, row 13), the subsequent iterations result in variable differentiation of the structure-type probabilities for the same data set with different confidence levels. The vertical lines represent ranges of structure-type probabilities when different orders of iteration are chosen. In Fig. 9, two orders of iterations are presented; one starts with the information concerning the strongest relative weighting factor and then proceeds downward (Table 1, iteration number 1 to 13; data represented in Fig. 9 by symbols); the second order of iterations starts with the information on the weakest relative weighting factor and then proceeds upward (Table 1, iteration number 13 to 1; data represented in Fig. 9 by the tops of the vertical lines). A confidence factor of 0.9 for the drill-core layer results in a GG classification with a probability of more than 70%. A factor of confidence of 0.9 reflects a high degree of confidence in the drill-core description (e.g. due to detailed drill-core analysis based on the Unified Soil Classification System (USCS: Wagner, 1957) and additional sedimentological attributes). A factor of confidence of 0.5 indicates a lower degree of confidence in the drill-core description (e.g. due to bad drill-core analysis or washing by flushing fluids during drilling).

Interpretation of GPR data

Ground-penetrating radar data (e.g. reflection profiles) provide two-dimensional images that permit the division of the subsurface into zones of more and less prominent reflection patterns. According to the interpretation concepts of Hardage (1987), Beres and Haeni (1991) and Huggenberger (1993), a radar facies type can be defined as a mappable sedimentary structure with a reflection pattern differing from those in adjacent structures. The geometry of the sedimentary structure types can be delineated by more continuous reflections and the types of reflection patterns within a certain visible structure. In addition, an angular unconformity between prominent reflections can be an indicator of an erosional surface, which separates different sedimentary units.

Transformation of the reflections from travel-time to depth requires information on the velocity distribution. The velocity field of the GPR waves is derived using the common midpoint method (CMP). Semblance velocity analysis (e.g. Beres *et al.*, 1999) shows that interval velocities in gravel deposits range from 0.07 m ns^{-1} to 0.11 m ns^{-1}

Table 1 Sedimentological information in drill-core layer descriptions and relative weighting factors with indications of the sedimentary structure type, for which the information is typical. OW, open framework well-sorted gravel; OW/BM, open framework well-sorted/bimodal gravel couplets; GG, grey gravel; BG, brown gravel; GG/BG-horizontal, alternating grey and brown gravel, horizontally layered; GG/BG-inclined, alternating grey and brown gravel, inclined; SG, silty gravel; SA, sand; SI, silt. The colour separation above and below –5.0 m arises from the different geology of the source areas: above –5.0 m the deposits consist exclusively of Wiese gravel, below –5.0 m the deposits consist of Rhine and subordinate quantities of Wiese gravel

Sedimentological information *(Iteration number)*		Typical sedimentary structure types	Relative weighting factor
Major constituent *(1)*	Silt	SI	1
	Sand	SA	
	Gravel	OW, OW/BM, GG, BG, GG/BG-h/-i, SG	
Quantity of (clay)–silt–(sand) *(3)*	Clean	OW, OW/BM, GG, GG/BG-h/-i, SA	0.7
	Little silt/silty	BG, GG/BG-h, GG/BG-i, SA	
	Little silt and sand	OW, OW/BM	
	Much silt/clay	SG	
Quantity of sand *(4)*	Little sand, 3–15%	OW/BM, BG, SG, SI	0.7
	Abundant sand, 16–30%	GG, BG, GG/BG-h/-i, SG	
	Much sand, 31–49%	GG, SG, SA	
Quantity of gravel *(10)*	Little gravel, 3–15%	SA, SI	0.25
	Abundant gravel, 16–30%	SA, SI	
	Much gravel, 31–49%	SA, SI	
Quantity of cobbles *(11)*	Few cobbles	OW/BM, GG, BG, GG/BG-h/-i, SG, SA	0.25
	Abundant cobbles	GG, BG, GG/BG-h/-i	
	Many cobbles	BG	
Fraction of sand *(5)*	Fine sand	BG, GG/BG-h/-i, SA, SI	0.55
	Medium sand	OW/BM, GG, BG, GG/BG-h/-i, SG, SA	
	Coarse sand	OW/BM, GG, SA	
Fraction of gravel *(8)*	Fine gravel	GG, SG, SA, SI	0.4
	Medium gravel	OW, OW/BM, GG, GG/BG-h/-i, SA	
	Coarse gravel	OW/BM, BG, GG/BG-h/-i	
Open framework gravel *(2)*	Open framework gravel	OW, OW/BM	0.85
	Fe-/Mg-precipitation	OW, OW/BM	
Sorting of sand *(6)*	Well sorted	OW/BM, GG, SA	0.55
	Poorly sorted	OW, BG, GG/BG-h/-i, SG, SA	
Sorting of gravel *(9)*	Well sorted	OW, OW/BM, SA	0.4
	Poorly sorted	GG, BG, GG/BG-h/-i, SG, SA	
Colour *(7)* (above –5 m)	Grey	OW, OW/BM, GG	0.55
	Brown	GG, BG, SG, SA, SI	
	Grey-brown	GG, BG, GG/BG-h/-i, SG, SA, SI	
Colour *(7)* (below –5 m)	Grey	OW, OW/BM, GG, SG, SA, SI	
	Brown	BG	
	Grey-brown	GG/BG-h/-i, SA	
Thickness of layer *(12)*	Thin, <0.25 m	OW	0.25
	Normal, 0.25–2.5 m	OW/BM, GG, BG, GG/BG-h/-i, SG, SA, SI	
	Thick, >2.5 m	BG	
Underlying layer *(13)*	SA	SI	0.1
	OW, OW/BM, GG	BG, GG/BG-h/-i, SG	
	BG, GG/BG-h/-i, SI, SG	OW, OW/BM, GG, SA	

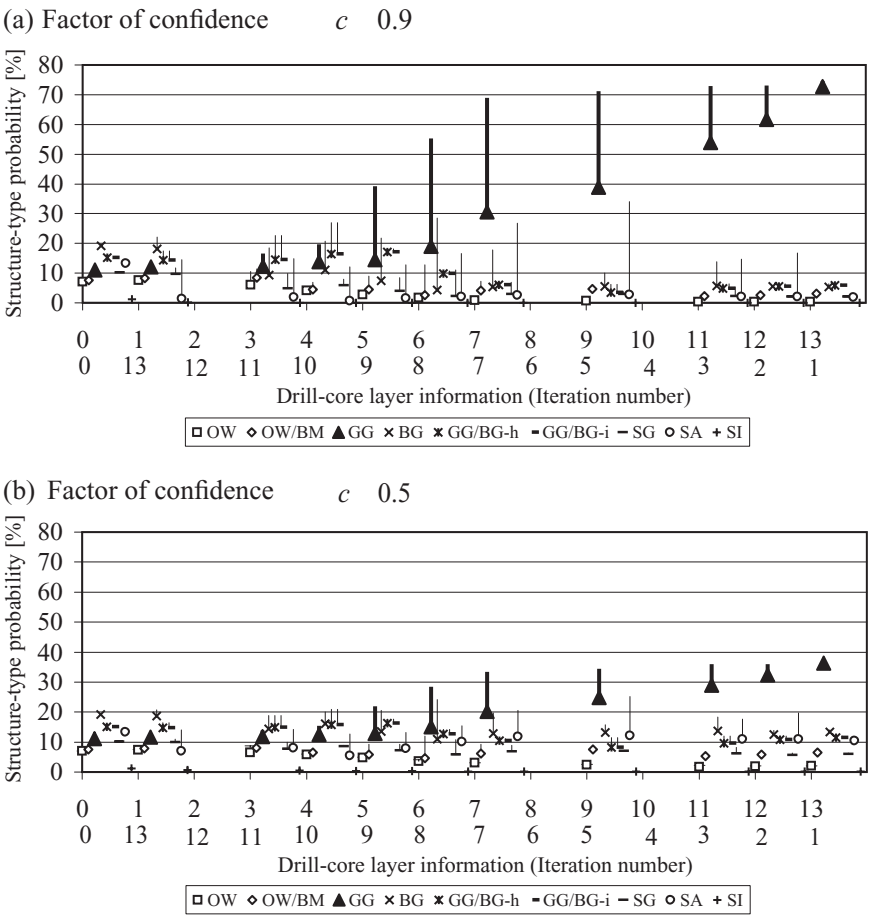

Fig. 9 Differentiation of sedimentary structure-type probabilities (%) based on the integration of sedimentological drill-core layer information and the factor of confidence in the drill-core description. Data shown are for layer 5 from borehole 1477 (see Regli *et al.*, 2002): (a) high confidence in drill-core description; (b) moderate confidence in drill-core description. The fine vertical lines represent ranges of structure-type probabilities when different orders of integration of layer information are chosen. See text for explanation.

(mean at 0.095 m ns^{-1}) for the different CMPs. Depending on the velocity field, linear or more complex velocity functions have to be considered for the transformation of the reflections from travel-time to depth. Due to the accuracy of the vertical resolution, which is equal to a quarter of the applied GPR wavelength, and the variance of the wave velocity in comparison to the resolution of the lithological units in drill cores, a constant velocity is assumed as a first approximation. For more complex velocity functions, calibration curves need to be considered, which transform individual boundaries from two-way travel-time to depths by using interpolation schemes for differing neighbouring velocity logs (Copty & Rubin, 1995).

The radar facies types can be calibrated based on interpreted drill cores located in the vicinity of GPR sections. The calibration process consists of assigning the calculated structure-type probabilities of the drill-core layer descriptions to the corresponding radar facies types. The mathematical details of this method are described in Regli *et al.* (2002). Figure 10a provides an example of oblique sigmoidal and oblique parallel radar facies types within a portion of a GPR section that incorporates borehole 1462 (Rhine/Wiese aquifer; see Regli *et al.*, 2002). The difference in thickness suggested by drill-core layers and the GPR structures depends on the resolution of the visual drill-core analysis (usually to a few centimetres) and the frequency used in GPR mapping (usually to a few decimetres for 50 MHz antennae).

Drill-core and GPR data processing

For the application of drill-core and GPR data to subsurface aquifer modelling, one-dimensional drill-core data and the two-dimensional images of GPR sections have to be transformed into point data. Data processing is necessary once facies analysis is performed. The lithofacies-based interpretation of drill-core and GPR data based on Regli *et al.*

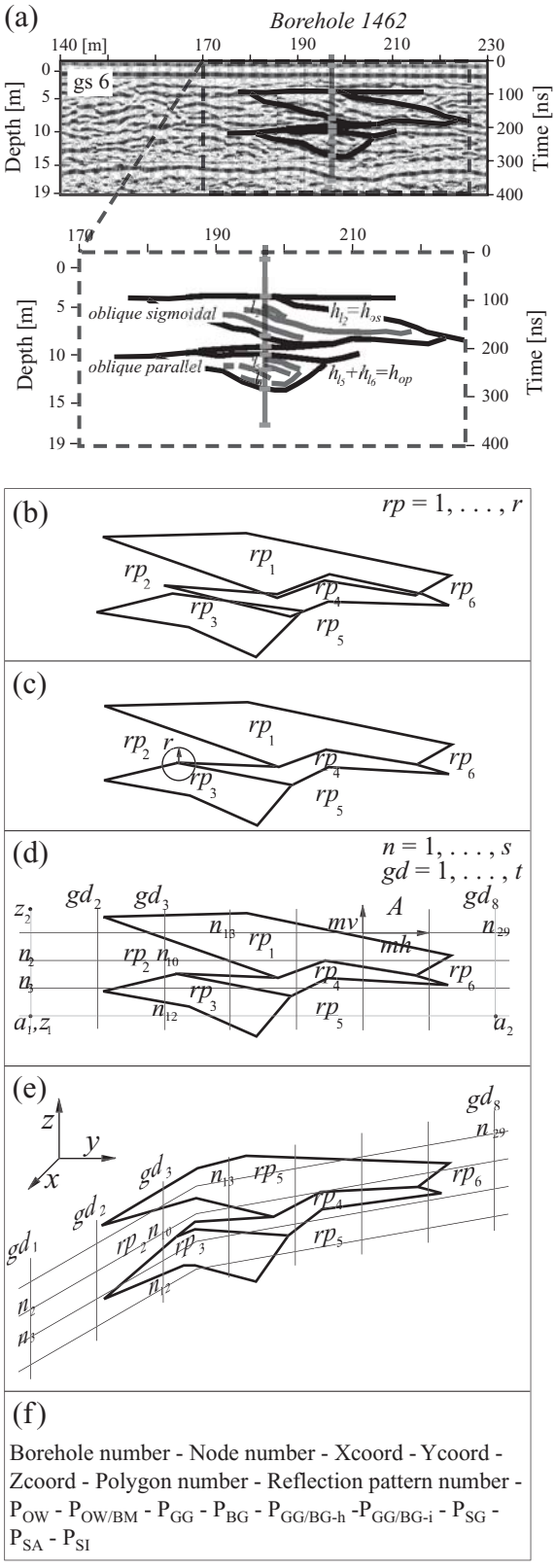

(2002) considers differences in data uncertainty and provides lithofacies probabilities for given points along boreholes and grid nodes with arbitrary mesh sizes along GPR sections. The processing steps for the GPR data are schematically shown in Fig. 10b–f. The procedure consists of (i) digitizing reflection pattern boundaries (Fig. 10b), (ii) snapping common points of neighbouring polygons (GPR structures; Fig. 10c), (iii) rasterizing polygons and generating nodes (grid-points; Fig. 10d), (iv) transforming relative coordinates into absolute coordinates (Fig. 10e) and (v) assigning data to nodes (Fig. 10f).

The digitization of the reflection patterns ($rp = 1, \ldots, r$) is carried out with digicps-3, an appended digitizing software for CPS-3 (Radian Corporation, 1992). Usually the points of neighbouring polygons are not coincident. For successive data processing steps, supplemental program routines were written in C. The snapping tool allows input of the radius (r) into which polygon points will be snapped. The rasterizing tool allows the input of the area of the GPR section ($A = a_1, a_2, z_1, z_2$) to be rasterized and the input of the horizontal (mh) and vertical (mv) mesh sizes between nodes. Nodes ($n = 1, \ldots, s$) with the same a coordinates (direction along GPR profile) but various z coordinates (depth) are grouped into a 'GPR borehole' ($gd = 1, \ldots, t$). The data density has to be chosen in such a way that GPR structures are clearly shown. The coordinate transformation tool changes relative two-dimensional coordinates (a,z) into absolute three-dimensional coordinates (x,y,z). Finally, the assigning tool allows the arrangement of all information such as data source (GPR or borehole),

Fig. 10 (*left*) A graphical summary of the steps used in radar facies analysis and data processing: (a) assignment of sedimentary structure-type probabilities from drill-core layer descriptions to corresponding radar facies types according to the proportion in thickness between drill-core layer and GPR structure; (b) digitizing GPR pattern boundaries; (c) snapping of common polygon points; (d) rasterizing polygons and generating nodes (grid-points); (e) transforming relative coordinates into absolute coordinates; (f) assigning information (e.g. physical parameters) to nodes. gs, GPR section; rp, reflection pattern; r, radius; n, node; gd, 'GPR borehole'; mh, horizontal mesh size; mv, vertical mesh size; A, area of GPR section (gs; A: a_1,a_2,z_1,z_2); P, probability of sedimentary structure type.

borehole number, node number, x, y and z coordinates, depth, polygon number, reflection pattern number, detail of whether a node is a surface node or not, probabilities of the sedimentary structure types OW, OW/BM, GG, BG, GG/BG-h, GG/BG-i, SG, SA, and SI to the corresponding nodes. The data are in a comma-separated-value (CSV) format, with each node in a separate line and each kind of information separated by a comma. Subsurface modelling software requires spatial coordinates (x,y,z) as well as data such as sedimentary structure types, probability details, hydraulic and geotechnical parameters obtained at the nodal location.

EXAMPLE OF STOCHASTIC AQUIFER SIMULATION USING HARD AND SOFT DATA

Simulation software and project integration

The mathematical tool GEOSSAV (Geostatistical Environment for Subsurface Simulation And Visualization) can be used for the integration of hard and soft data, and in the three-dimensional stochastic simulation and visualization of the distribution of geological structures and hydrogeological properties in the subsurface (Regli *et al.*, 2004). The tool GEOSSAV can be used for data analysis, variogram computation of regularly or irregularly spaced data, and sequential indicator simulation of subsurface heterogeneities when employed as an interface to selected geostatistical programs from the Geostatistical Software Library, GSLIB (Deutsch & Journel, 1998). Simulations can be visualized by three-dimensional rendering and slicing perpendicular to the main coordinate axis. The data can then be exported into regular grid-based groundwater simulation systems (e.g. ASMWIN (Chiang *et al.*, 1998); GMS (Environmental Modelling Systems Inc., 2002); PMWIN (Chiang & Kinzelbach, 2001)).

In the current study, GEOSSAV was used to generate the sedimentary structures and hydraulic aquifer properties in the vicinity of a drinking water well. The simulated aquifer properties were integrated into a 550 m × 400 m × 21 m, 11-layer finite-difference groundwater flow and transport model to simulate a river restoration pilot project near a well-field in a gravel aquifer supplying the city of Basel (Fig. 1). Groundwater simulation of this portion of the Rhine/Wiese aquifer is of interest since it includes simulations of changing well capture zones depending on the sedimentary structures present in the subsurface, hydrological variations, the operating regime of the drinking water wells, and the progress of river restoration activities (Regli *et al.*, 2003). The aim of the following example is to demonstrate the different steps followed in the characterization of subsurface heterogeneity, depending on the proposed sedimentological model and the geostatistical analysis employed using the available data.

Field data of different quality

The study site is located at the ancient confluence where the River Rhine flowed to the northwest and its tributary, the River Wiese, flowed to the southwest (Fig. 1). The average discharge of the River Rhine at this location over the past 110 yr was 1052 $m^3 s^{-1}$, and the discharge of the Rhine is around 90 times larger than the average discharge of the Wiese (11.4 $m^3 s^{-1}$, based on measurements collected over the past 68 yr (Swiss Federal Office for Water and Geology, 2001)). Rhine and Wiese sediments are lithologically distinct from each other as the two rivers derived their sediments from two geologically different catchment areas. Within these two lithological units, a number of sedimentary structures are recognized that were generated by sedimentary processes operating in braided rivers. Lithofacies associated with the sedimentary structures at this location include (Regli *et al.*, 2002): OW, OW/BM, GG, BG, GG/BG, as well as horizontally layered or inclined, and SG, SA and SI. Drill-core data from five boreholes and GPR data from 14 vertical GPR sections (total length of all sections is 3040 m; GPR line orientations within the field of 550 m × 400 m are given in Fig. 11) indicated that the unconfined aquifer consists of coarse unconsolidated Quaternary alluvial deposits. Tertiary marls underlie these gravels and are considered impermeable for the purposes of the model simulations. Aquifer thickness varies between 13 and 18 m. The lower 80% of the aquifer consists of Rhine gravel (primarily limestone) and the upper 20% of the aquifer consists of Wiese gravel (primarily silicates and limestone; Zechner *et al.*, 1995). These lithological differences may be explained by the River Rhine reworking the Wiese gravel

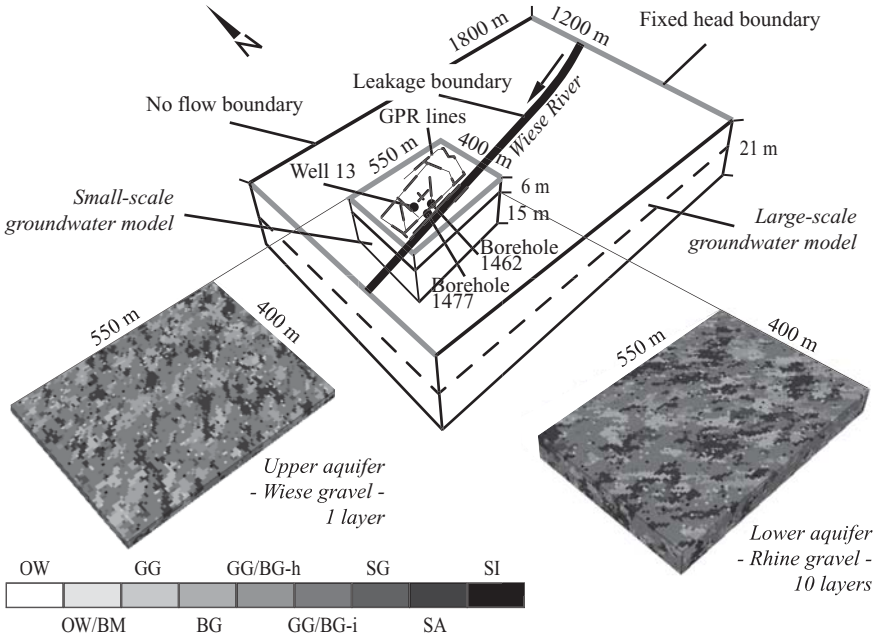

Fig. 11 Location of the small-scale groundwater model within a large-scale homogeneous groundwater model. The small-scale model relies on stochastically generated aquifer properties. OW, open framework well-sorted gravel; OW/BM, open framework well-sorted/bimodal gravel couplets; GG, grey gravel; BG, brown gravel; GG/BG-h, alternating grey and brown gravel, horizontally layered; GG/BG-i, alternating grey and brown gravel, inclined; SG, silty gravel; SA, sand; SI, silt.

at very high flow stages, whereas the uppermost part of the Wiese gravel sequence was preserved until the next shift of the active channel of the Rhine. The data sampled from the GPR sections are given for nodes with 5 m lateral spacing along the profile direction and 1 m vertical spacing.

Variogram computation

Modelling spatial variability of data is the key to any subsurface simulation. A variogram describes the spatial correlation of data as a function of the separation vector between two data points. The indicator variogram computation was based on the drill-core and GPR data described above, and was run separately for the lower part (Rhine gravel) and the upper part (Wiese gravel) of the aquifer. The indicator transform (Deutsch & Journel, 1998) at grid node locations was set to unity for structure types with the greatest probability values, but otherwise was zero. Experimental indicator variograms were calculated for various directions (azimuth, dip, plunge). Table 2 presents the resulting parameters for the nine sedimentary structure types identified at the study site. Azimuth (both dip and plunge are 0°) and the ranges corresponding to maximum and minimum horizontal and vertical spatial correlation distances characterize the geometric anisotropy of the sedimentary structure types.

The results of the variogram analysis provide the orientation of the sedimentary structure types representing the main flow direction of the River Rhine in the lower part, and of the River Wiese in the upper part of the aquifer, respectively. The relatively large ranges of spatial correlation, ranging from a few metres up to a few tens of metres for the different sedimentary structure types (Table 2), may be significantly influenced by the resolution of the GPR system and the density of the sampled data taken from the GPR sections. The sedimentary structures of the Rhine gravel were modelled as geostatistical structures that are around 20% and 45% larger in the horizontal and vertical directions respectively compared with the structures of the Wiese gravel.

Aquifer simulation

The aquifer structure was simulated by sequential indicator simulation (Deutsch & Journel, 1998; Regli *et al.*, 2004). The sequential indicator simulation principle is an extension of conditioning that includes all data available within the neighbourhood of a model cell, including the original data and all previously simulated values. Sequential

Table 2 Rhine gravel and Wiese gravel parameters used for the sequential indicator simulation to define the geometric anisotropy of the sedimentary structure types: OW, open framework well-sorted gravel; OW/BM, open framework well-sorted/bimodal gravel couplets; GG, grey gravel; BG, brown gravel; GG/BG-horizontal, alternating grey and brown gravel, horizontally layered; GG/BG-inclined, alternating grey and brown gravel, inclined; SG, silty gravel; SA, sand; SI, silt. Values in italics are estimates; the isotropic nugget constants of the sedimentary structure types are zero; the variogram models of the sedimentary structure types are exponential; the dip and plunge of the sedimentary structure types are zero degrees; the sill refers to the positive variance contribution in the variogram model (Deutsch & Journel, 1998)

	Parameter	Sedimentary structure type								
		OW	OW/BM	GG	BG	GG/BG horizontal	GG/BG inclined	SG	SA	SI
Wiese gravel	Volumetric fraction (%)	*0.02*	0.05	0.16	0.05	*0.50*	*0.05*	0.02	0.14	*0.01*
	Sill (–)	*0.13*	0.12	0.18	0.115	*0.13*	*0.13*	0.045	0.18	*0.13*
	Azimuth (°)	*240*	240	240	240	*240*	*240*	270	200	*240*
	Maximum horizontal range (m)	*3*	24	60	34	*50*	*7*	14	50	*3*
	Minimum horizontal range (m)	*1.5*	18	24	24	*18*	*3*	18	16	*1.5*
	Vertical range (m)	*0.5*	4	6	5	*6*	*1*	4	3	*0.5*
Rhine gravel	Volumetric fraction (%)	*0.02*	0.06	0.12	0.05	*0.50*	*0.05*	0.03	0.16	*0.01*
	Sill (–)	*0.1*	0.095	0.155	0.055	*0.1*	*0.1*	0.04	0.17	*0.1*
	Azimuth (°)	*310*	320	315	300	*310*	*310*	300	300	*310*
	Maximum horizontal range (m)	*5*	54	60	40	*70*	*8*	30	60	*5*
	Minimum horizontal range (m)	*2*	22	19	22	*30*	*4*	17	22	*2*
	Vertical range (m)	*1*	10	5	11	*10*	*2*	10	8	*1*

indicator simulations are processed in a number of steps. An initial step establishes a grid network and coordinate system, and this is followed by assigning data to the nearest grid node. Where more than one data point may be used at a node, the closest data point is assigned to the grid node. In a third step, a random path through all grid nodes is determined. For a node on a random path, adjacent data and previously simulated grid nodes are searched, to permit an estimation of the conditional distribution by indicator kriging. Based on this distribution, a simulated lithofacies is randomly drawn and set as hard data before the next node in the random path is selected and the process repeated. By using this approach, the simulation grid is built up sequentially. During the final step of the sequential indicator simulation, results are checked to ensure that orientations and sizes of the simulated sedimentary structures are in accordance with those observed.

The one sequential indicator simulation, using separate runs for the lower and the upper parts of the aquifer, is presented in Fig. 11. The regular model grid is defined by $110 \times 80 \times 10$ cells for the lower part and by $110 \times 80 \times 1$ cells for the upper part of the aquifer, respectively. Cell sizes are $5\,m \times 5\,m \times 1.5\,m$ for the lower part, and $5\,m \times 5\,m \times 6\,m$ for the upper part, respectively. Each simulated sedimentary structure-type distribution is termed an aquifer realization. In each model run, the resulting probability density functions of the sedimentary structure types deviate less than ±10% from the initial probability density functions, which represent the expected volumetric fractions of the sedimentary structure types over the entire model domain (see Table 2; Jussel *et al.*, 1994). In order to determine statistical moments and their confidence limits by Monte Carlo type modelling, a minimum of 100 or 1000 runs are necessary. The changes in orientation and ranges of possible sedimentary structures, caused by the above-mentioned interactions of the two rivers over time, are recognized and included in the model by partitioning the aquifer vertically into two hydrostratigraphic units.

The sedimentary structures generated are characterized by randomly selecting hydraulic conductivity and porosity values provided from means and standard deviations calculated by Jussel *et al.* (1994). Files containing distributions of hydraulic conductivity and effective porosity values were generated and exported to a Modflow-based groundwater simulation system, in order to perform groundwater flow and transport simulations (PMWIN, Chiang & Kinzelbach, 2001). This process is described in detail in Regli *et al.* (2003). Groundwater flow and transport simulations are in accordance with field measurements including tracer breakthrough concentrations and groundwater head measurements. Each aquifer simulation represents various equiprobable representations of the subsurface with a variable degree of uncertainty in hydraulic parameter values and geometry of sedimentary structures, as based on the aquifer sedimentological and geostatistical analyses.

DISCUSSION

Sedimentary texture and structure types along with depositional elements of sedimentological models can be observed in almost all Pleistocene fluvial deposits in Switzerland as well as many other braided river systems (e.g. Steel & Thompson, 1983; Ramos *et al.*, 1986; Heinz, 2001). The similarities in characteristic grain-size distributions and hydraulic conductivities of deposits from different Pleistocene rivers have been documented by Jussel (1992). Similarities in grain-size curves were also found when comparing the gravel-sheet deposits of modern rivers with samples observed in gravel pits or drill cores (Nägeli *et al.*, 1996; Regli *et al.*, 2002). Sedimentary texture and structure types of a former inactive floodplain can be observed only at very few locations in the uppermost metres of the Rhine valley deposits between the Alpine front and Basel. The sedimentary structure types observed in the former floodplain are largely irrelevant for hydrogeological applications because the water table is generally below these units.

It is uncertain whether the difference between bounding-surface models dominated by horizontal and trough-shaped boundary surfaces could be attributed to two different braided river systems, for the following reasons.

1 The dynamic character of braided rivers determines the preservation potential of the different depositional elements, and hence the spatial extent of the different sedimentary structure types in the geo-

logical record. In rivers with low aggradation rates and high bedload-sheet activities, scour fills have the highest chance of being preserved. An example of the dominance of OW/BM is documented in the Marthalen system (Fig. 5), where more than 60% of the deposits consist of scour fills. In rivers with high aggradation rates and low gravel-sheet activities, gravel sheets have a higher probability of being preserved.

2 Although it can be documented from many outcrops and GPR surveys that the horizontally dominated bounding surfaces are most abundant in the uppermost metres (Huggenberger *et al.*, 1998; Carling *et al.*, 2000), this may not be due to major differences in their depositional system. The dominance of horizontal bounding surfaces near the top of the deposits may be explained by (i) incision of the main channels of a stream (lowering of the base level) during normal runoff, including high flow stages, followed by (ii) broadening of the valley bottom by lateral erosion accompanied by minor deposition during occasional events of very high runoff (landscape shaping events) by the end of late Pleistocene. Such a shift would subsequently stop fluvial activity in the higher terrace levels. Consequently, when examining sedimentary structures in Pleistocene deposits, the dominance of horizontal bounding surfaces may be restricted to the uppermost part of the outcrop sections. This in turn implies that, when examining modern fluvial environments, an exploration depth of the geophysical method of at least the deepest scour is required to fully describe the bounding surfaces.

Bluck (1979), Steel & Thompson (1983), Lunt & Bridge (2004) and Lunt *et al.* (2004) provided descriptions of horizontally layered sediments overlaying tangentially dipping cross-beds, separated by erosional surfaces. Their observations suggest processes acting at two different vertical levels. Ashmore (1982), when studying the initiation of braiding in a straight channel in a laboratory flume, also found that each individual bar was associated with a local scour immediately upstream. The relative importance of scour pools in braided river deposits has also been shown in previous investigations by Ashmore (1993) and Bristow & Best (1993). Ashmore (1982) concluded that any attempt to explain the development of a braided pattern from alternating bars must account for scours, and that alternating bars and scours are interrelated. Scours in alluvial systems related to gravel sheets develop over distances that are up to several times bankfull channel width (Lewin, 1976; Tubino *et al.*, 1999; Lanzoni, 2000; Church, 2002). The scours associated with gravel sheets develop and fill with the advance of gravel sheets, while the fill process is completed only during waning flow. Due to the turbulent, turbid water during high flow, the scour cut-and-fill process was not observed in the Madonna del Ponte outcrop in the Tagliamento River. However, scour structures can be portrayed by GPR profiling, and the sedimentary texture types in the central part of a gravel sheet have been shown to mainly consist of poorly to moderately sorted gravel ranging from coarse sand to cobbles with almost no silt and clay.

The example of the Tagliamento River provides some insight into the mechanisms of sediment sorting during flooding (high flow). Figure 7 illustrates a transition from an avalanche face of a gravel sheet into a scour. The transition represents a negative step, which may produce a flow separation zone (Best & Roy, 1991; Best, 1993). With an angle of about 90°, inclined gravel dunes migrating across the lateral scour wall produce smaller-scale secondary flow separation zones. The migration of several gravel dunes across the lateral trough wall might be explained by a sequence of sediment pulses, as recognized by Klingemann & Emmett (1982) and more recent flume experiments (e.g. Marti, 2002). However, a more continuous sediment supply cannot be excluded, although this has not been recorded under comparable experimental conditions. According to Carling & Glaister (1987) and Carling (1990), negative steps may lead to the formation of gravel couplets, which represent a fining-upward sequence of BM at the base and OW at the top. An advance of several migrating small gravel dunes across the lateral trough walls concurs with the results of numerical models of confluence dynamics (Bradbrook *et al.*, 2000), which allow visualization of flow vectors when overpassing negative steps (e.g. the situation at the front of gravel dunes). Models of confluence dynamics have been compared with the results of laboratory experiments and field data (Rhoads, 1996; Rhoads & Kenworthy, 1998), and predictions of flow in cross-sectional planes portray a rotational flow and an upward component of the flow in the scour (Bradbrook *et al.*, 2000). This flow pattern

is consistent with the upward-migrating gravel dunes along the flank of the scour that produce tangential sets of OW/BM. A possible link between the processes described above and the resulting sedimentary structures in a vertical profile perpendicular to the mean ancient flow direction is presented in Fig. 4d. Contrary to that which might be expected from a first inspection of a trough fill consisting of sets with OW/BM cross-beds, these cross-beds could develop by migration of gravel dunes across the lateral trough walls.

Drill-core layer descriptions generally represent mixtures of different sedimentary structure types and often only sparse indications of OW strata can be identified in drill-core layer descriptions. Nevertheless, it is evident from many recent outcrop observations that OW and OW/BM occur frequently (Siegenthaler & Huggenberger, 1993). Consequently, hydrogeological models based on drill-core data may reproduce effective hydraulic conductivities, but underestimate their standard deviations. This underestimation may be critical when transport distances of particles or microorganisms in heterogeneous aquifers need to be evaluated. A fruitful subject of future research would be to investigate what percentage of OW strata are required to affect the hydrogeological, statistical characteristics of a deposit.

The ability to integrate different quality data, such as outcrop and drill-core analysis, geophysical methods and geostatistical data, into mathematical models offers a great potential for improving the accuracy of aquifer models. This is particularly relevant when considering the integration of drill-core and two-dimensional or three-dimensional structure information from GPR data into groundwater flow and transport models, especially when considering the variable degree of uncertainty associated with estimating the hydraulic properties and geometry of the sedimentary structures. Textural and structural interpretations of GPR data are fuzzy to some extent, and this results in a probability estimate that drill-core layer descriptions and radar facies types represent defined sedimentary structure types. These structure-type probabilities can be given for points along boreholes, and grid nodes with arbitrary mesh sizes along GPR sections. In order to derive maximum benefit from available textural and structural information, sequential indicator simulation techniques have been used to simulate the distributions of subsurface geological structures and their associated hydrogeological properties. Based on variogram modelling and the choice of the simulation routine, various equiprobable realizations have to be generated to provide an objective, statistically supported view of reality.

CONCLUSIONS

1 The approach used to characterize aquifer heterogeneity presented in this paper considers the differences between lithofacies-based interpretation of outcrop, drill-core and GPR data. The lithofacies scheme is based on observations of unsaturated sand and gravel outcrops and fluvio-dynamic interpretations of processes in a braided river. This approach is suitable for the interpretation of radar facies types. Moreover, the analysis of a large number of vertical sections in gravel pits and construction sites (e.g. Figs 1–5) in Switzerland, France and southern Germany has shown that trough-shaped erosional surfaces are the dominant sedimentary features. In contrast, horizontal gravel sheets were encountered less frequently than expected, based on modern analogues (e.g. Lunt *et al.*, 2004). The trough-fill deposits seen in gravel pits represent the infilling of ancient scour pools.

2 Observations and GPR experiments at different locations in the Pleistocene Rhine gravel deposits of Switzerland show that scour dimensions vary according to the palaeodischarge, as well as the width of the active channel belt or the valley (Beres *et al.*, 1999). Two-dimensional and three-dimensional GPR data may be used to estimate the scour-fill/channel-fill ratio and the proportion of other deposits present, and time slices of three-dimensional GPR experiments can provide maps of the ancient fluvial systems at different depths (Beres *et al.*, 1999). Both data types are of particular interest when studying aquifer heterogeneity.

3 Observations in gravel pits and on the River Tagliamento raise questions concerning the validity of the widely accepted assumption among sedimentologists that the description of modern analogues permits the essence of the heterogeneity of a deposit to be ascertained. By following this rationale, the role of scour fills containing open framework well-sorted (OW) and open framework well-sorted/bimodel (OW/BM) gravel might be at least underestimated,

or even overlooked. When addressing many hydrogeological issues related to gravel aquifers, the most important structure types are OW and OW/BM. The extent of these highly permeable sediments is related to the dimensions of the depositional trough-fill deposits. A dominance of trough-fill deposits has also been recorded based on three-dimensional GPR investigations (Beres *et al.*, 1999). Vertical GPR sections may be used to estimate the scour-fill/channel-fill ratio, and to characterize the geometry of the erosional surfaces of sedimentary structures and their radar facies types.

4 Application of the procedures outlined in this paper provides a means of integrating different quality data. The approach results in a simulated aquifer model that includes quantifiable uncertainty associated with the quantity and quality of data parameter values. This uncertainty must be considered in both assigning values to parameters and in the identification of particular structures. The application of stochastic methods based on reliable sedimentological models therefore provides an objective means of handling both hard and soft data associated with large-scale subsurface heterogeneities.

ACKNOWLEDGEMENTS

We thank K. Bernet and R. Flynn for reviewing the manuscript. Special thanks are addressed to J. Best, J. Bridge, I. Lunt, G. Weissman and J. West for valuable critiques and comments that have significantly improved the manuscript. This study was supported by the Swiss National Science Foundation, grant no. 2100-049272.96/1. The C routines referred to in this paper are available on request from the authors.

REFERENCES

Adams, E.E. and Gelhar, L.W. (1992) Field study of dispersion in a heterogeneous aquifer, 2, Spatial moment analysis. *Water Resour. Res.*, **28**, 3293–3308.

Anderson, M.P. (1989) Hydrogeologic facies models to delineate large-scale spatial trends in glacial and glaciofluvial sediments. *Geol. Soc. Am. Bull.*, **101**, 501–511.

Anderson, M.P., Aiken, J.S., Webb, E.K. and Mickelson, D.M. (1999) Sedimentology and hydrogeology of two braided stream deposits. *Sediment. Geol.*, **129**, 187–199.

Allen, J.R.L. (1978) Studies in fluviatile sedimentation: An exploratory quantitative model for the architecture of avulsion-controlled alluvial suits. *Sediment. Geol.*, **21**, 129–147.

Allen, J.R.L. (1984) Parallel lamination developed from upper-stage plane beds: a model based on the larger coherent structures of the turbulent boundary layer. *Sediment. Geol.*, **39**, 227–242.

Ashmore, P.E. (1982) Laboratory modelling of gravel braided stream morphology. *Earth Surf. Process.*, **7**, 2201–2225.

Ashmore, P. and Parker, G. (1983) Confluence scour in coarse braided streams. *Water Resour. Res.*, **19**, 392–402.

Ashmore, P. (1993) Anabranch confluence kinetics and sedimentation processes in gravel braided streams. In: *Braided Rivers* (Eds J.L. Best and C.S. Bristow), pp. 129–146. Special Publication 75, Geological Society Publishing House, Bath.

Ashworth, P.J., Best, J.L., Peakall, J. and Lorsong, J.A. (1999) The influence of aggradation rate on braided alluvial architecture: field study and physical scale modelling of the Ashburton River gravels, Canterbury Plains, New Zealand. In: *Fluvial Sedimentology VI* (Eds N.D. Smith and J. Rogers), pp. 333–346. Special Publication 28, International Association of Sedimentologists. Blackwell Science, Oxford.

Ashworth, P.J., Best, J.L. and Jones, M. (2004) The relationship between sediment supply and avulsion frequency in braided rivers. *Geology*, **32**, 21–24.

Asprion, U. and Aigner, T. (1999) Towards realistic aquifer models: three-dimensional georadar surveys of Quaternary gravel deltas (Singen Basin, SW Germany). *Sediment. Geol.*, **129**, 281–297.

Beres, M. and Haeni, F.P. (1991) Application of ground-penetrating radar methods in hydrogeologic studies. *Groundwater*, **29**, 375–386.

Beres, M., Green, A.G., Huggenberger, P. and Horstmeyer, H. (1995) Mapping the architecture of glaciofluvial sediments with three-dimensional georadar. *Geology*, **23**, 1087–1090.

Beres, M., Huggenberger, P., Green, A.G. and Horstmeyer, H. (1999) Using two- and three-dimensional georadar methods to characterise glaciofluvial architecture. *Sediment. Geol.*, **129**, 1–24.

Best, J.L. (1993) On the interactions between turbulent flow structure, sediment transport and bedform development: some considerations from recent experimental research. In: *Turbulence: Perspectives on Flow and Sediment Transport* (Eds N.J. Clifford, J.R. French and J. Hardisty), pp. 61–92. Wiley, Chichester.

Best, J.L. and Roy, A.G. (1991) Mixing layer distortion at the confluence of channels of different depth. *Nature*, **350**, 411–413.

Best, J.L., Ashworth, P.J., Bristow, C. and Roden, J. (2003) Three-dimensional sedimentary architecture of a large, mid-channel sand braid bar, Jamuna River, Bangladesh. *J. Sediment. Res.*, **73**, 516–530.

Bluck, B.J. (1979) Structure of coarse grained braided stream alluvium. *Trans. Roy. Soc. Edinb.*, **70**, 181–221.

Bradbrook, K.F., Lane, S.N. and Richards, K.S. (2000) Numerical simulation of three dimensional, time averaged flow structure at river channel confluences. *Water Resour. Res.*, **36**, 2731–2746.

Brierley, G.J. (1991) Bar sedimentology of the Squamish river, British Columbia: definition and application of morphostratigraphic units. *Journal of Sedimentary Petrology*, **61**, 211–225.

Bridge, J.S. (1993) The interaction between channel geometry, water flow, sediment transport and deposition in braided rivers. In: *Braided Rivers* (Eds J.L. Best and C.S. Bristow), pp. 13–71. Special Publication 75, Geological Society Publishing House, Bath.

Bridge, J.S. (2003) *Rivers and Floodplains*. Blackwell Scientific, Oxford, 504 pp.

Bridge, J.S., Alexander, J., Collier, R.E.L.L., Gawthorpe, R.L. and Jarvis, J. (1995) Ground-penetrating radar and coring to study the large-scale structure of point-bar deposits in three dimensions. *Sedimentology*, **42**, 839–852.

Bristow, C. and Best, J.L. (1993) Braided rivers: perspectives and problems. In: *Braided Rivers* (Eds J.L. Best and C.S. Bristow), pp. 1–9. Special Publication 75, Geological Society Publishing House, Bath.

Carle, S.F., LaBolle, E.M., Weissmann, G.S., Van Brocklin, D. and Fogg, G.E. (1998) Conditional simulation of hydrofacies architecture: A transition probability/Markov approach. In: *Hydrogeologic Models of Sedimentary Aquifers* (Eds G.S. Fraser and J.M. Davis), pp. 147–170. Concepts in Hydrogeology and Environmental Geology 1, Society of Economic Paleontologists and Mineralogists,Tulsa, OK.

Carling, P.A. (1990) Particle over-passing on depth-limited gravel bars. *Sedimentology*, **37**, 345–355.

Carling, P.A. and Glaister, M.S. (1987) Rapid depositions of sand and gravel mixtures downstream of a negative step: the role of matrix-infilling and particle overpassing in the process of bar-front accretion. *J. Geol. Soc. London*, **144**, 543–551.

Carling, P.A., Gölz, E., Orr, H.G. and Radecki-Pawlik, A. (2000) The morpholodynamics of fluvial sand dunes in the River Rhine, near Mainz, Germany. I. Sedimentology and morphology. *Sedimentology*, **47**, 227–252.

Chiang, W.-H. and Kinzelbach, W. (2001) *3D-Groundwater Modelling with PMWIN—a Simulation System for Modeling Groundwater Flow and Pollution*. Springer, Berlin, 346 pp.

Chiang, W.-H., Kinzelbach, W. and Rausch, R. (1998) *Aquifer Simulation Model for Windows—Groundwater Flow and Transport Modeling, an Integrated Program*. Gebrueder Borntraeger, Berlin, 137 pp.

Church, M. (2002) Geomorphic thresholds in riverine landscapes. *First International Symposium on Landscape Dynamics of Riverine Corridors*, Ascona, Switzerland, March, 2001. *Freshwat. Biol.*, **47**, 541–557.

Copty, N. and Rubin, Y. (1995) A stochastic approach to the characterisation of lithofacies from surface seismic and well data. *Water Resour. Res.*, **31**, 1673–1686.

Dagan, G. (2002) An overview of stochastic modelling of groundwater flow and transport: from theory to applications. *Eos (Trans. Am. Geophys. Soc.)*, **83/53**, 621–625.

Deutsch, C.V. and Wang, L. (1996) Hierarchical object-based stochastic modelling of fluvial reservoirs. *Math. Geol.*, **28**, 857–880.

Deutsch, C.V. and Journel, A.G. (1998) *GSLIB Geostatistical Software Library and User's Guide*. Oxford University Press, New York, 369 pp.

Environmental Modelling Systems Inc. (2002) *GMS: Groundwater Modelling System*. http://www.ems-i.com.

Fay, H. (2002) Formation of ice-block obstacle marks during the November 1996 glacier-outburst flood (Jökulhlaup), Skeidarársandur, southern Island. In: *Flood and Megaflood Processes and Deposits: Recent and Ancient Examples* (Eds I.P. Martini, V.R. Baker and G. Garzón), pp. 85–97. Special Publication 32, International Association of Sedimentologists. Blackwell Science, Oxford.

Flynn, R. (2003) *Virus transport and attenuation in perialpine gravel aquifers*. Unpublished PhD thesis, University of Neuchâtel, Switzerland, 178 pp.

Fogg, G.E., Noyes, C.D. and Carle, S.F. (1998) Geologically based model of heterogeneous hydraulic conductivity in an alluvial setting. *Hydrogeol. J.*, **6**, 131–143.

Gelhar, L.W. (1986) Stochastic subsurface hydrology from theory to applications. *Water Resour. Res.*, **22**, 135S–145S.

Hardage, B.A. (1987) *Seismic Stratigraphy*. Geophysical Press, London, 422 pp.

Heller, P. and Paola, C. (1992) The large-scale dynamics of grain-size variation in alluvial basins, 2: application to syntectonic conglomerate. *Basin Res.*, 4, 73–90.

Heinz, J. (2001) *Sediment. Geol. of Glacial and Periglacial Gravel Bodies (SW-Germany): Dynamic Stratigraphy and Aquifer Sedimentology*. Tübinger Geowissenschaftliche Arbeiten, C59, 102 pp.

Huggenberger, P. (1993) Radar facies: recognition of facies patterns and heterogeneities within Pleistocene Rhine gravels, NE Switzerland. In: *Braided Rivers* (Eds J.L. Best and C.S. Bristow), pp. 163–176. Special

Publication 75, Geological Society Publishing House, Bath.

Huggenberger, P., Siegentaler, C. and Stauffer, F. (1988) Grundwasserströmung in Schottern: Einfluss von Ablagerungsformen auf die Verteilung von Grundwasserfliessgeschwindigkeit. *Wasserwirtschaft*, **78**, 202–212.

Huggenberger, P., Höhn, E. and Beschta, R. (1998) Groundwater control on riparian/fluvial systems. *Freshwat. Biol.*, **40**, 407–425.

Jussel, P. (1992) *Modellierung des Transports gelöster Stoffe in inhomogenen Grundwasserleitern*. Unpublished PhD thesis, 9663. Eidgenössisch Technische Hochschule, Zürich, 323 pp.

Jussel, P., Stauffer, F. and Dracos, T. (1994) Transport modelling in heterogeneous aquifers: 1. statistical description and numerical generation of gravel deposits. *Water Resour. Res.*, **30**, 1803–1817.

Klingbeil, R., Kleineidam, S., Asprion, U., Aigner, T. and Teutsch, G. (1999) Relating lithofacies to hydrofacies: outcrop-based hydrogeological characterisation of Quaternary gravel deposits. *Sediment. Geol.*, **129**, 299–310.

Klingemann, P.C. and Emmett, W.W. (1982) Gravel bedload transport processes. In: *Gravel-bed Rivers* (Eds R.D. Hey, J.C. Bathurst and C.R. Thorne), pp. 145–169. Wiley, Chichester.

Koltermann, C.E. and Gorelick, S.M. (1992) Paleoclimate signature in terrestrial flood deposits. *Science*, **256**, 1775–1782.

Koltermann, C.E. and Gorelick, S.M. (1996) Heterogeneity in sedimentary deposits: A review of structure-imitating, process-imitating, and descriptive approaches. *Water Resour. Res.*, **32**, 2617–2658.

Leopold, L.B. and Wolman, M.G. (1957) River channel patterns, braided, meandering, straight. *US Geol. Surv. Prof. Pap.*, **282-B**.

Lanzoni, S. (2000) Experiments on bar formation in a straight flume 1. Uniform sediment. *Water Resour. Res.*, **36**(11), 3351–3363.

Lewin, J. (1976) Initiation of bed forms and meanders in coarse-grained sediment. *Geol. Soc. Am. Bull.*, **87**, 281–285.

Lunt, I.A. and Bridge, J.S. (2004) Evolution and deposits of a gravelly braid bar, Sagavanirktok River, Alaska. *Sedimentology*, **51**, 415–432.

Lunt, I.A., Bridge, J.S. and Tye, R.S. (2004) A quantitative, three-dimensional depositional model of gravelly braided rivers. *Sedimentology*, **51**, 377–414.

Marti, C. (2002) Morphodynamics of widenings in steep rivers. In: *River Flow 2002* (Eds D. Bousmar and Y. Zech), Vol. 2, pp. 865–873. A.A. Balkema, Lisse.

McKenna, S.A. and Poeter, E.P. (1995) Field example of data fusion in site characterization. *Water Resour. Res.*, **31**, 3229–3240.

Miall, A.D. (1985) Architectural-element analysis: a new method of facies analysis applied to fluvial deposits. *Earth Sci. Rev.*, **22**, 261–308.

Nägeli, M.W., Huggenberger, P. and Uehlinger, U. (1996) Ground penetrating radar for assessing sediment structures in the hyporheic zone of a perialpine river. *J. N. Am. Benthol. Soc.*, **15**, 353–366.

Paola, C., Heller, P. and Angevine, C. (1992) The large-scale dynamics of grain-size variation in alluvial basins, 1: Theory. *Basin Res.*, **4**, 73–90.

Radian Corporation (1992) *CPS-3, User's Manual*. Radian Corporation, Austin, London.

Ramos, A., Sopeña, A. and Perez-Arlucea, M. (1986) Evolution of Buntsandstein fluvial sedimentation in the north-west Iberian ranges (Central Spain). *J. Sediment. Petro.*, **56**, 862–875.

Rauber, M., Stauffer, F., Huggenberger, P. and Dracos, T. (1998) A numerical three-dimensional conditioned/unconditioned stochastic facies type model applied to a remediation well system. *Water Resour. Res.*, **34**, 2225–2233.

Regli, C., Huggenberger, P. and Rauber, M. (2002) Interpretation of drill-core and georadar data of coarse gravel deposits. *J. Hydrol.*, **255**, 234–252.

Regli, C., Rauber, M. and Huggenberger, P. (2003) Analysis of heterogeneity within a well capture zone, comparison of model data with field experiments: a case study from the river Wiese, Switzerland. *Aquat. Sci.*, **65**, 111–128.

Regli, C., Rosenthaler, L. and Huggenberger, P. (2004) GEOSSAV: a simulation tool for subsurface applications. *Comput. Geosci.*, **30**, 221–238.

Rehfeldt, K.R., Boggs, J.M. and Gelhar, L.W. (1993) Field study of dispersion in a heterogeneous aquifer, 3, Geostatistical analysis of hydraulic conductivity. *Water Resour. Res.*, **28**, 3309–3324.

Rhoads, B.L. (1996) Mean structure of transport-effective flows at an asymmetrical confluence when the main stream is dominant. In: *Coherent Flow Structures in Open Channels* (Eds P.J. Ashworth, S.J. Bennett, J.L. Best and S.J. McLelland), pp. 459–490. Wiley, Chichester.

Rhoads, B.L. and Kenworthy, S.T. (1998) Time-averaged flow structure in the central region of a stream confluence. *Earth Surf. Process. Landf.*, **23**, 171–191.

Siegenthaler, C. and Huggenberger, P. (1993) Pleistocene Rhine gravel: deposits of a braided river system with dominant trough preservation. In: *Braided Rivers* (Eds J.L. Best and C.S. Bristow), pp. 147–162. Special Publication 75, Geological Society Publishing House, Bath.

Stauffer, F. and Rauber, M. (1998) Stochastic macrodispersion models for gravel aquifers, *J. Hydraul. Res.*, **36**, 885–896.

Steel, R.J. and Thompson, D.B. (1983) Structures and textures in Triassic braided stream conglomerates ('Bunter Pebble Beds') in the Sherwood Sandstone Group, North Staffordshire, England. *Sedimentology*, **30**, 341–367.

Swiss Federal Office for Water and Geology (2001) *The Hydrological Yearbook of Switzerland 2000*. Geneva, 432 pp.

Swiss Standard Association (1997) *Identifikation der Lockergesteine—Labormethode mit Klassifikation nach USCS (SN 670008a)*. Geneva, 7 pp.

Todd, S.P. (1989) Stream-driven, high-density gravelly traction carpets: possible deposits in the Trabeg Conglomerate formation, SW Ireland and some theoretical considerations on their origin. *Sedimentology*, **36**, 513–530.

Tubino, M., Repetto, R. and Zolezzi, G. (1999) Free bars in rivers. *J. Hydraul. Res.*, **37**, 759–775.

Van Dyke, M. (1982) *An Album of Fluid Motion*. Parabolic Press, Stanford, CA, 176 pp.

Wagner, A.A. (1957) The use of the Unified Soil Classification System by the Bureau of Reclamation. *Proceedings of the 4th International Conference on Soil Mechanics and Foundation Engineering*, Vol. 1, pp. 125–134.

Webb, E.K. (1994) Simulating the three-dimensional distribution of sediment units in braided-stream deposits. *J. Sediment. Res.*, **B64**, 219–231.

Webb, E.K. and Anderson, M.P. (1996) Simulation of preferential flow in three-dimensional, heterogeneous conductivity fields with realistic internal architecture. *Water Resour. Res.*, **32**, 533–545.

Weissmann, G.S., Carle, S.F. and Fogg, G.E. (1999) Three-dimensional hydrofacies modelling based on soil surveys and transition probability geostatistics. *Water Resour. Res.*, **35**, 1761–1770.

Zechner, E., Hauber, L., Noack, Th., Trösch, J. and Wülser, R. (1995) Validation of a groundwater model by simulating the transport of natural tracers and organic pollutants. In: *Tracer Technologies for Hydrological Systems* (Ed. Ch. Leibundgut), pp. 57–64. IAHS Publication 229, International Association of Hydrological Sciences, Wallingford.